
Article:
(2023) Advances and new ideas for neutron-capture astrophysics experiments at CERN n_TOF. European Physical Journal A. 8. ISSN: 1434-601X

https://doi.org/10.1140/epja/s10050-022-00876-7

Eur. Phys. J. A (2023) 59:8
https://doi.org/10.1140/epja/s10050-022-00876-7

THE EUROPEAN PHYSICAL JOURNAL A

Regular Article - Experimental Physics

Advances and new ideas for neutron-capture astrophysics experiments at CERN n_TOF

C. Domingo-Pardo[1,a], V. Babiano-Suarez[1], J. Balibrea-Correa[1], L. Caballero[1], I. Ladarescu[1], J. Lerendegui-Marco[1], J. L. Tain[1], A. Tarifeño-Saldivia[1], O. Aberle[2], V. Alcayne[3], S. Altieri[4], S. Amaducci[5], J. Andrzejewski[6], M. Bacak[2], C. Beltrami[4], S. Bennett[7], A. P. Bernardes[2], E. Berthoumieux[8], M. Boromiza[9], D. Bosnar[10], M. Caamaño[11], F. Calviño[12], M. Calviani[2], D. Cano-Ott[3], A. Casanovas[12], F. Cerutti[2], G. Cescutti[13,14], S. Chasapoglou[15], E. Chiaveri[2,7], N. M. Chiera[25], P. Colombetti[16], N. Colonna[17], P. Console Camprini[18], G. Cortés[12], M. A. Cortés-Giraldo[19], L. Cosentino[5], S. Cristallo[20,21], S. Dellmann[22], M. Di Castro[2], S. Di Maria[23], M. Diakaki[15], M. Dietz[24], R. Dressler[25], E. Dupont[8], I. Durán[11], Z. Eleme[26], S. Fargier[2], B. Fernández[19], B. Fernández-Domínguez[11], P. Finocchiaro[5], S. Fiore[27], F. García-Infantes[29], A. Gawlik-Ramięga [6], G. Gervino[16], S. Gilardoni[2], E. González-Romero[3], C. Guerrero[19], F. Gunsing[8], C. Gustavino[30], J. Heyse[31], W. Hillman[7], D. G. Jenkins[32], E. Jericha[33], A. Junghans[34], Y. Kadi[2], K. Kaperoni[15], F. Käppeler[28,†], G. Kaur[8], A. Kimura[35], I. Knapová[36], U. Köster[43], M. Kokkoris[15], M. Krtička[36], N. Kyritsis[15], C. Lederer-Woods[37], G. Lerner[2], A. Manna[18,38], T. Martínez[3], A. Masi[2], C. Massimi[18,38], P. Mastinu[39], M. Mastromarco[17,40], E. A. Maugeri[25], A. Mazzone[17,41], E. Mendoza[3], A. Mengoni[27], P. M. Milazzo[13], I. Mönch[45], R. Mucciola[20], F. Murtas[30,†], E. Musacchio-Gonzalez[39], A. Musumarra[5,44], A. Negret[9], A. Pérez de Rada[3], P. Pérez-Maroto[19], N. Patronis[26], J. A. Pavón-Rodríguez[19], M. G. Pellegriti[5], J. Perkowski[6], C. Petrone[9], E. Pirovano[24], J. Plaza[3], S. Pomp[42], I. Porras[29], J. Praena[29], J. M. Quesada[19], R. Reifarth[22], D. Rochman[25], Y. Romanets[23], C. Rubbia[2], A. Sánchez[3], M. Sabaté-Gilarte[2], P. Schillebeeckx[31], D. Schumann[25], A. Sekhar[7], A. G. Smith[7], N. V. Sosnin[37], M. Stamati[26], A. Sturniolo[16], G. Tagliente[17], D. Tarrío[42], P. Torres-Sánchez[29], J. Turko[34], S. Urlass[34,2], E. Vagena[26], S. Valenta[36], V. Variale[17], P. Vaz[23], G. Vecchio[5], D. Vescovi[22], V. Vlachoudis[2], R. Vlastou[15], T. Wallner[34], P. J. Woods[37], T. Wright[7], R. Zarrella[18,38], P. Žugec[10], The n_TOF Collaboration[,b]

[1] Instituto de Física Corpuscular, CSIC—Universidad de Valencia, Spain
[2] European Organization for Nuclear Research (CERN), Geneva, Switzerland
[3] Centro de Investigaciones Energéticas Medioambientales y Tecnológicas (CIEMAT), Madrid, Spain
[4] Laboratori Nazionali di Pavia, Pavia, Italy
[5] Istituto Nazionali di Fisica Nucleare (INFN), Sezione di Catania, Italy
[6] University of Lodz, Lodz, Poland
[7] University of Manchester, Manchester, UK
[8] CEA Irfu, Université Paris-Saclay, Paris, France
[9] Horia Hulubei National Institute of Physics and Nuclear Engineering, Magurele, Romania
[10] Department of Physics, Faculty of Science, University of Zagreb, Zagreb, Croatia
[11] University of Santiago de Compostela, Santiago De Compostela, Spain
[12] Universitat Politècnica de Catalunya, Catalonia, Spain
[13] Istituto Nazionale di Fisica Nucleare, Sezione di Trieste, Rome, Italy
[14] Osservatorio Astronomico di Trieste, Trieste, Italy
[15] National Technical University of Athens, Athens, Greece
[16] Laboratori Nazionali di Torino, Turin, Italy
[17] Istituto Nazionale di Fisica Nucleare, Sezione di Bari, Bari, Italy
[18] Istituto Nazionale di Fisica Nucleare, Sezione di Bologna, Bologna, Italy
[19] Universidad de Sevilla, Sevilla, Spain
[20] Istituto Nazionale di Fisica Nucleare, Sezione di Perugia, Perugia, Italy
[21] Istituto Nazionale di Astrofisica - Osservatorio Astronomico di Teramo, Teramo, Italy
[22] Goethe University Frankfurt, Frankfurt am Main, Germany
[23] Instituto Superior Técnico, Lisbon, Portugal
[24] Physikalisch-Technische Bundesanstalt (PTB), Braunschweig, Germany
[25] Paul Scherrer Institut (PSI), Villigen, Switzerland
[26] University of Ioannina, Ioannina, Greece
[27] Agenzia nazionale per le nuove tecnologie (ENEA), Bologna, Italy
[28] Karlsruhe Institute of Technology, Karlsruhe, Germany

[29] University of Granada, Granada, Spain
[30] Laboratori Nazionali di Frascati, Frascati, Italy
[31] European Commission, Joint Research Centre (JRC), Geel, Belgium
[32] University of York, York, United Kingdom
[33] TU Wien, Atominstitut, Wien, Austria
[34] Helmholtz-Zentrum Dresden-Rossendorf, Dresden, Germany
[35] Japan Atomic Energy Agency (JAEA), Tokai-Mura, Japan
[36] Charles University, Prague, Czech Republic
[37] School of Physics and Astronomy, University of Edinburgh, Edinburgh, United Kingdom
[38] Dipartimento di Fisica e Astronomia, Università di Bologna, Bologna, Italy
[39] Istituto Nazionale di Fisica Nucleare, Sezione di Legnaro, Italy
[40] Dipartimento Interateneo di Fisica, Università degli Studi di Bari, Bari, Italy
[41] Consiglio Nazionale delle Ricerche, Bari, Italy
[42] Uppsala University, Uppsala, Sweden
[43] Institut Laue Langevin, Grenoble, France
[44] Dipartimento di Fisica e Astronomia, Università di Catania, Catania, Italy
[45] Leibniz-Institut für Festkörper- und Werkstoffforschung Dresden (IFW) e.V., Dresden, Germany
† Deceased

Received: 4 August 2022 / Accepted: 31 October 2022 / Published online: 26 January 2023

Communicated by N. Alamanos

Abstract This article presents a few selected developments and future ideas related to the measurement of (n, γ) data of astrophysical interest at CERN n_TOF. The MC-aided analysis methodology for the use of low-efficiency radiation detectors in time-of-flight neutron-capture measurements is discussed, with particular emphasis on the systematic accuracy. Several recent instrumental advances are also presented, such as the development of total-energy detectors with γ-ray imaging capability for background suppression, and the development of an array of small-volume organic scintillators aimed at exploiting the high instantaneous neutron-flux of EAR2. Finally, astrophysics prospects related to the intermediate *i* neutron-capture process of nucleosynthesis are discussed in the context of the new NEAR activation area.

1 Introduction

The fundamental role of neutron-induced reactions in the formation of the heavy elements in the universe was already evident in 1948 [1–4], although it was probably the first observation of technetium in S-type stars [5] and the subsequent quantitative theory of nucleosynthesis [6,7], which triggered and guided an enormous experimental effort, that still prevails today [8–14]. This article describes some experimental developments primarily aimed at measuring nuclear data of interest for nucleosynthesis studies in hydrostatic stages of stellar evolution, namely asymptotic giant branch (AGB-) and massive-stars [10,15]. These works were carried out at the n_TOF facility, which has been extensively described in detail elsewhere [16–18]. The first topic reported in Sect. 2 is related to the accuracy of the measurements carried out in neutron time-of-flight (TOF) experiments using low-efficiency radiation detectors. This is an important subject for astrophysics because data from many previous measurements still exhibit cross-section uncertainties that are significantly larger than the few percent uncertainty attainable from stellar observations or meteorites analysis [10]. The experimental situation is illustrated in Fig. 1, which shows Maxwellian average cross sections (MACS) at $kT = 30$ keV and current uncertainties [19] for all nuclei involved in *s*-process nucleosynthesis. As pointed out in several recent sensitivity studies [20–24], the cross sections of many isotopes need to be re-measured either with improved accuracy or over more complete neutron-energy ranges in order to derive reliable information of astrophysical interest. This is particularly true for the seeds of the *s* process around the Fe-Ni region [21], whose cross sections at $kT = 30$ keV still show relatively large uncertainties (see bottom panel in Fig. 1). For this reason, many neutron-capture experiments were made in the Fe/Ni region at n_TOF [13,25–28], JRC-Geel [29], Los Alamos National Laboratory [30,31] and elsewhere [32]. Following this logic, many more experiments on stable isotopes will still follow in the coming years. The new measurements will benefit, not only from the enhanced accuracy approach described below in Sect. 2, but also from new instrumental developments such as those reported in Sects. 3 and 4.

Another topic which focuses many experimental efforts nowadays is the determination of neutron-capture cross sections on unstable nuclei [10]. In AGB- and massive stars, radioactive nuclei may split the nucleosynthesis path and

[a] e-mail: domingo@ific.uv.es (corresponding author)
[b] https://www.cern.ch/ntof

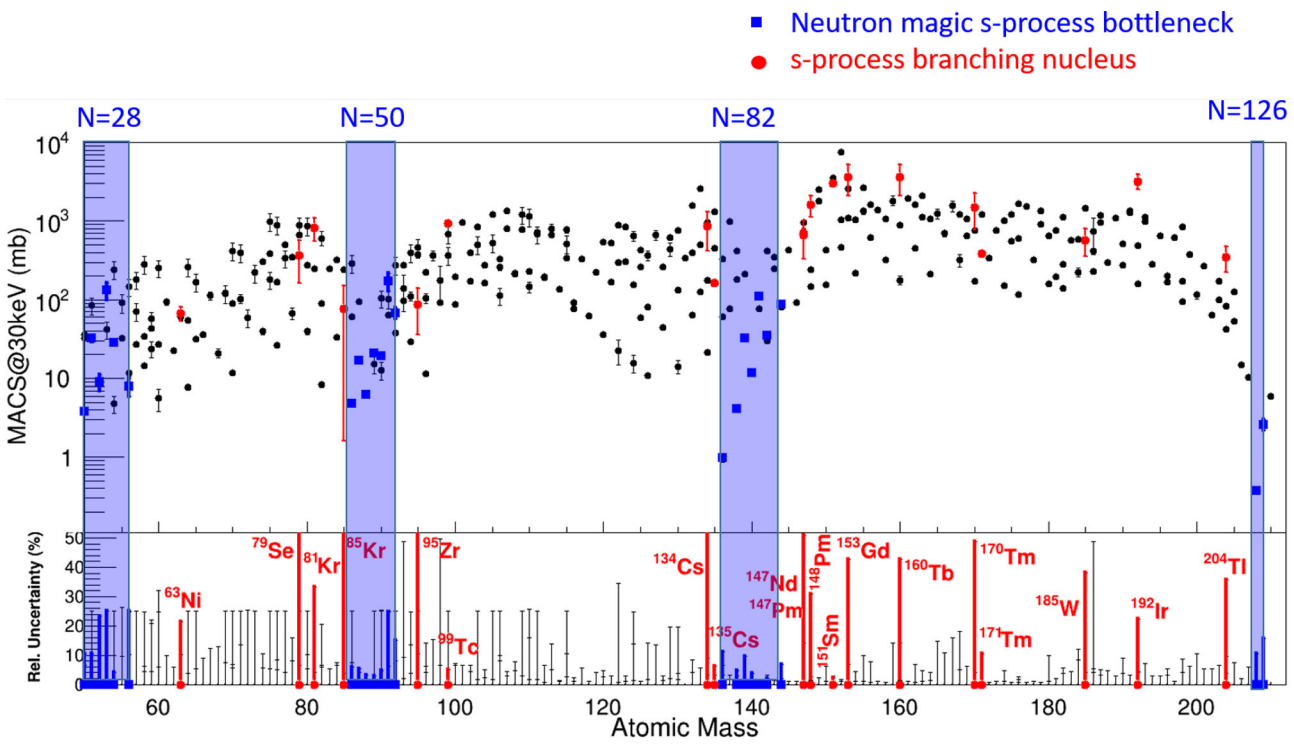

Fig. 1 Maxwellian averaged neutron-capture cross section at $kT = 30$ keV (top panel) and their relative uncertainties (bottom panel). Blue colors refer to nuclei with neutron-shell closures and branching nuclei are displayed in red. Most values are taken from [19] (see text for details)

yield a local isotopic pattern around the branching nucleus, which is very sensitive to the physical conditions of the stellar environment. Therefore, neutron-capture measurements of these nuclei provide stringent constraints on stellar structure and evolution models. As shown in Fig. 1 several *s*-process branching nuclei have been measured with high accuracy [10,13], but there is still a significant number of them that have not been accessed yet owing to limitations in state-of-the-art detection systems and sample-production capabilities. Sections 3 and 4 describe some recent technical developments aimed at enhancing detection sensitivity in neutron-capture experiments, either by means of γ-imaging or by means of very-low efficiency detectors. Section 5 then describes new ideas at n_TOF intended to afford direct neutron-capture measurements of interest for more exotic stellar environments, such as the intermediate *i*-process of nucleosynthesis [33]. Finally, Section 6 summarizes the main conclusions and future prospects.

2 Improved accuracy measurements via MC-aided PHWT

One of the most relevant aspects when dealing with experimental data concerns the systematic accuracy of the measurement, the proper identification of experimental uncertainties and their realistic assessment. Therefore, in the first n_TOF experimental campaign in 2001 a study [34] was carried out in order to address the systematic accuracy attainable with the so-called Pulse-Height Weighting Technique (PHWT). Originally developed in the sixties at ORNL in a pioneer work by Macklin et al. [35], the PHWT has been extremely helpful and very extensively used at different laboratories worldwide for the determination of neutron-capture data of astrophysical interest [8,10]. The Total-Energy Detection (TED) principle in combination with the PHWT allowed one to virtually mimic an ideal Moxon-Rae detector [36]. However, the new approach was much more flexible in terms of apparatus and permitted to attain higher efficiency and better detection sensitivity [8]. The latter was a key aspect to access neutron-capture reactions of astrophysical relevance [35], including also radioactive isotopes such as the *s*-process branchings ^{93}Zr [37] and ^{99}Tc [38].

An interesting aspect of the TED principle applied with the PHWT is the fact that, essentially, only the requirement of using low-efficiency γ-ray detectors needs to be experimentally fulfilled [35]. This opens up a wide scope of options in terms of instrumentation, an aspect that has been also explored and exploited at n_TOF during the last years, as described later in Sects. 3 and 4. Obviously, other additional conditions are required for neutron-TOF experiments, such as fast time-response and low intrinsic sensitivity to scattered neutrons.

However, for several decades the systematic accuracy attainable with the PHWT was a topic of controversy and debate. As clearly stated by Corvi [39], one of the most

puzzling aspects in the eighties was a 20% discrepancy between capture- and transmission-measurements found for the 1.15 keV resonance in ^{56}Fe(n,γ). At that time, this was quoted as "one of the four major outstanding neutron data problems in the field of fission reactor neutronics" [40]. The 1.15 keV resonance in ^{56}Fe represents indeed an ideal case for testing the accuracy of the technique because the capture TOF experiment is mainly sensitive to the neutron width Γ_n, which is accurately known from transmission measurements [41].

In order to tackle this challenge and eventually develop a general and reliable methodology for the analysis of capture data with the PHWT, at n_TOF we carried out a detailed Monte-Carlo study [42] followed by a series of systematic measurements [34]. The latter involved the use of two different C_6D_6 detectors and iron samples of three different thicknesses (from 0.5 mm to 2 mm). The general conclusions of this work were essentially two. First, it was understood that the only reliable methodology to apply the PHWT accurately was by means of detailed and realistic Monte Carlo (MC) simulations of the experimental set-up for the determination of the weighting function (WF), which included also a specific simulation for every particular sample used in the capture experiments. Thus, at variance with the original approach [35] and later works [39,43], there is not such a thing like "The weighting function of the C_6F_6 scintillation detector" [43–45] or a unique "experimental WF" [39]. Instead, a WF needs to be calculated for each capture set-up and for each specific sample measured in the TOF experiment [34]. For relatively thick samples a resonance-dependent WF may be needed in order to account for the different γ-ray emission and absorption profiles across the sample thickness [46]. This effect was relevant, for example, in the measurement of ^{197}Au(n,γ) [47] or ^{232}Th(n,γ) [48]. Self-shielding effects can also play an important role for some samples or resonances and, therefore, the methodology developed in Ref. [46] has been included in the R-matrix analysis code REFIT [49]. For a recent review on the analysis techniques for neutron induced reaction cross-section data the reader is referred to Ref. [50].

The fact that the WF and the PHWT accuracy is so dependent on so many experimental details reflects also the level of sensitivity in these measurements, where small changes in the experimental conditions can be quickly reflected in the acquired capture data. The new MC-aided approach represented a change of paradigm in the analysis of neutron-capture data using the PHWT, which has been adopted by the scientific community [46,51]. It is worth to emphasize that the work reported in [39] and references therein, although did not provide a final solution to this problem, it had a crucial relevance towards understanding its origin. It is worth recalling also that MC simulations using the EGS-transport code were applied in ORNL already in 1988 [52]. However, the latter work still proposed a single WF for all capture experiments regardless of the sample characteristics.

The second aspect found in [34] to be of relevance for the accuracy of the PHWT was related to the signature of nuclear-structure effects in the response functions measured with the C_6D_6 detectors. In general, differences are found between the capture-cascade spectrum of the sample under study, and the one used as reference, commonly ^{197}Au(n,γ). The methodology proposed in Ref. [34] to account for this effect involves the MC simulation of the full capture cascade for both studied- and reference-samples, and then determine a yield correction factor. Because of the interplay with the nuclear-structure effects, the correction factor may even change from one capture-resonance to another, depending on the resonance spin and parity [53–55]. The main contributions to the yield-correction factor arise from the different number of counts missing under the detection threshold (typically 150–200 keV), γ-ray summing effects, angular-distribution effects [54,56], conversion-electrons and, if present, isomeric-states [53]. References quoted represent examples, where such correction factors were crucial to keep the systematic uncertainty within the level of 2–3% RMS. Finally, this result also highlights the relevance of suitable computing codes and libraries [57], methods and models [58–61] for simulating the cascade of prompt γ-rays in neutron-capture experiments.

3 Background suppression via γ-ray imaging

As discussed in the preceding section, one of the most striking features of the TED principle is related to its versatility, namely enabling the use of almost any detection system with efficiency low enough to satisfy

$$\varepsilon^c = 1 - \prod_{j=1}^{N}(1-\varepsilon_j^\gamma) \simeq \sum_{j=1}^{N}\varepsilon_j^\gamma . \tag{1}$$

Here, N is the number of emitted γ-rays, ε^c represents the capture-detection probability and ε^γ the γ-ray detection efficiency. In addition, the efficiency-energy proportionality, $\varepsilon_j^\gamma \propto E_j^\gamma$, required to attain the total cascade-energy response $\varepsilon^c \propto E^c$ can be achieved by means of the PHWT [35]. As mentioned before, the detector response function needs to be also suitable for neutron-TOF experiments. Aiming at reducing neutron-induced backgrounds in the detector itself, organic C_6F_6 detectors were used in the first experiments [35,39], which were later replaced by C_6D_6 further optimized by means of C-fiber encapsulations and other improvements [34,62].

Apart from organic scintillation detectors, a NaI(Tl) spectrometer has been used at ANNRI J-PARC [44,45,63,64], which actually demonstrates that it is possible to extend the

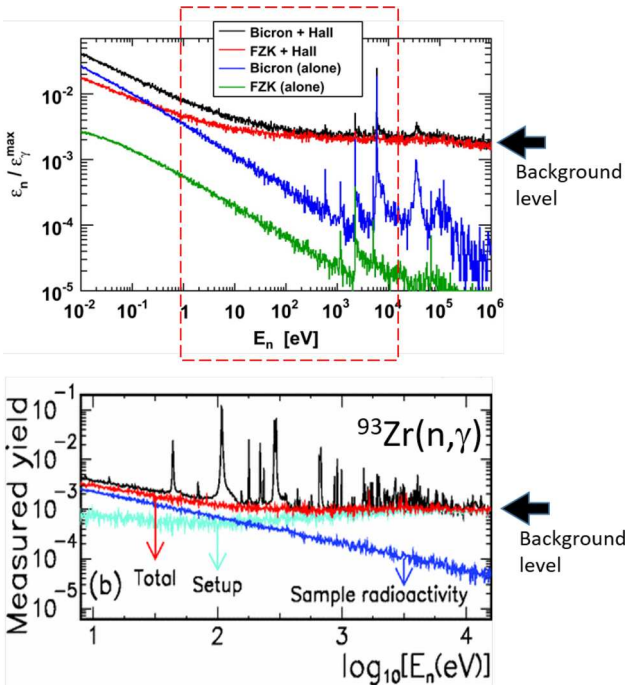

Fig. 2 (Top panel) MC simulation [25] of the neutron sensitivity, which shows the C_6D_6-response to neutron-induced γ-ray background in the walls of the experimental hall. In practice, the resonant structure in the 1–100 keV neutron-energy range is suppressed due to the loss of time-energy correlations for the scattered neutrons (see Ref. [67] for details). (Bottom panel) Capture yield of ^{93}Zr(n, γ) [66], which shows the limiting effect of the background level in the keV neutron-energy range

TED principle to very different types of detection systems. Exploiting further this aspect, a new approach has been investigated at n_TOF, which applies γ-ray imaging techniques to discriminate spatially localized γ-ray background sources [65]. This concept seems particularly interesting for the measurement of samples with a small neutron-capture cross section, where neutrons scattered in the sample and subsequently captured in the walls of the experimental hall dominate the background level, instead of neutrons captured directly in the detectors themselves. This situation is depicted in Fig. 2-top, which shows that in the keV neutron-energy region of astrophysical interest the background may be rather dominated by neutrons captured in the walls of the experimental hall, rather than in the detectors themselves [25]. The impact of this background is illustrated in Fig. 2-bottom with the measurement of ^{93}Zr(n, γ) performed at n_TOF [66]. As indicated in Ref. [20], improving the cross-section measurement could help to constrain even more the thermal conditions in AGB stars.

First attempts to apply γ-ray imaging techniques for background suppression in neutron-capture experiments at n_TOF employed a pin-hole γ-camera with a bulky lead collimator attached to a position-sensitive radiation detector [68]. This work actually demonstrated for the first time the possibility to incorporate imaging techniques in neutron-TOF experiments, although improvements were rather limited owing to the additional background induced by neutrons in the massive collimator itself. The problems ascribed to the use of a massive collimator could be fully overcome by means of an alternative technique based on electronic collimation, originally developed for γ-ray astronomy [69,70]. This new approach based on the Compton imaging technique [65] has been developed in the framework of the ERC-project HYMNS [71] during the last years at CERN n_TOF. Compton imaging is based on the use of two or more planes of radiation detectors with both energy- and position-sensitivity operated in time-coincidence. In this way, when a γ-ray undergoes interaction in several detectors the Compton scattering law can be applied in order to infer information on the incoming radiation direction. Several technical developments were necessary in order to adapt existing technologies to the field of neutron-capture measurements. These developments were mainly related to the need of achieving good enough energy resolution with SiPMs and large monolithic crystals [72], high spatial resolution and linearity that are challenging due to the big size of the scintillation crystals [73,74] and implementing a customized dynamic electronic-collimation method for enhanced performance in the Compton imaging [75].

Proof-of-principle experiments [76] have been performed at n_TOF with a prototype of a Total-Energy Detector with imaging capability, called i-TED. These measurements show a significant background reduction in the keV neutron-energy range of interest for astrophysics, when compared to state-of-the-art C_6D_6 detectors.

Figure 3 shows a picture of the final i-TED system for (n, γ) experiments, which consists of an array of four large-solid angle Compton cameras in a close configuration around the capture sample. Every Compton module comprises 5 inorganic scintillation crystals, each of them with a size of 50×50 mm^2. The front scatter position-sensitive detector has a thickness of 15 mm, whereas the four crystals in the rear absorber plane have a thickness of 25 mm. The modules have been designed in order to maximize detection efficiency, while minimizing neutron-sensitivity in the detectors themselves. To accomplish the latter goal $LaCl_3$(Ce) was preferred versus other options, owing to the relatively small integral capture cross section of Chlorine, and the small contribution of resonances in the keV-energy range of relevance. The Compton modules are supplemented with ^{6}Li neutron-absorber pads of 20 mm thicknes for reducing further the intrinsic neutron sensitivity of the array (see Fig. 3).

Pixelated silicon photomultipliers (SiPMs) are used for the readout of the 20 inorganic crystals, leading to a total number of 1280 readout channels. To cope with this large number a dedicated acquisition system based on ASIC TOFPET2 modules [77] was implemented and adapted to this type of

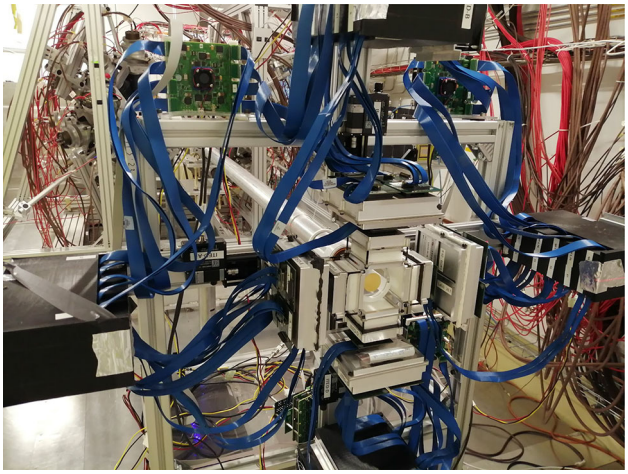

Fig. 3 Photograph of the i-TED array during a calibration measurement for the ^{79}Se(n,γ) experiment in 2022 at CERN n_TOF EAR1

experiments. For further details the reader is referred to Refs. [75,76] and references therein.

The i-TED array has been recently applied for the first measurement of the ^{79}Se(n,γ) capture cross section at n_TOF EAR1 [78]. A ^{79}Se sample was produced by high-fluence neutron irradiation in the V4 beam tube of the ILL reactor in Grenoble. To this aim, an eutectic PbSe-alloy sample was prepared at the Paul Scherrer Institut (PSI) in Switzerland, which allowed one to overcome the difficulties ascribed to the low melting point of selenium [79]. The measurement with the i-TED array in EAR1 was intended to reduce the large scattered-neutron background arising from the large lead content in the sample, 2.8 g. Furhter, the final PbSe sample had an activity of 5 MBq of ^{75}Se and 1.6 MBq of ^{60}Co. Therefore, this sample was also measured at the EAR2 station with the set-up described in the following section. ^{79}Se is an important *s*-process branching nucleus, which is particularly well suited to constrain the thermal conditions of the *s*-process in the weak *s* process [10,22,80]. Once fully analyzed, the results of this experiment will help to constrain the thermal conditions during core He-burning and shell C-burning in massive stars.

4 Small-volume C_6D_6 detectors with high rate capability

In situations where the background in the experiment is dominated by the decay radioactivity of the sample itself it may become more convenient to exploit the high instantaneous neutron-flux of the EAR2 measuring station. In this way, the relative contribution of the sample radioactivity is minimized with respect to the radiative-capture channel of interest. The large instantaneous neutron-flux of n_TOF EAR2 [81] is particularly well suited for these challenging cases. As described in [82], the high peak flux becomes one of the most important features when measuring radioactive samples because it allows for a reduction of the sample-activity background contribution relative to the time-interval where the neutron capture yield is measured. However, in order to exploit the large peak-neutron flux one requires also radiation detectors with a fast time-response and a high count-rate capability. State-of-the-art C_6D_6 detectors with a volume of $\sim$1 l [62] have a relatively large efficiency, which in turn requires a large sample-detector distance to avoid excessive signal pile-up and dead time arising from the high count-rate conditions of about 1 MHz, or more. Also, the i-TED system described in the preceding section is presently limited to count rates of about 500 kHz [77], owing to the ASIC-readout scheme implemented to cope with the 1280 readout channels of the twenty position-sensitive detectors. It is expected that future developments will help to enhance the ASIC event-rate capability and possibly, make the i-TED system also useful for measurements in the high-flux conditions of EAR2.

To overcome the count-rate limitations of conventional C_6D_6 detectors an array of nine small-volume (49 ml) C_6D_6 detectors [83], was implemented in a compact-ring configuration [84] around the capture sample in EAR2 as shown in Fig. 4. The main advantage of this innovative setup is that the small detection volume allows one to place the detectors much closer to the capture sample under study, and thus enhance also the efficiency for true capture γ-rays and increase the signal-to-background ratio (SBR) with respect to previous set-ups based on larger C_6D_6 detectors placed further away from the beam-line. The improvement in SBR is shown in the bottom panel of Fig. 4, which shows an enhanced signal-to-background ratio for the ^{197}Au(n,γ) reaction over most of the energy range when measured with the small-volume C_6D_6 detectors.

The set-up shown in Fig. 4 was used in the 2022 campaign for the measurement of the ^{94}Nb(n,γ) cross section [74]. The ^{94}Nb sample used for this TOF experiment was produced by high-fluence neutron irradiation of hyperpure niobium samples [85] in the V4 tube of the ILL-Grenoble reactor. The final sample contained a total amount of 9×10^{18} atoms with an activity dominated (10 MBq) by the β-decay of ^{94}Nb (2×10^4 y). The results from this experiment are expected to shed light on isotopic anomalies observed in pre-solar SiC grains [86], which apparently require an unexpectedly large *s*-process contribution to the abundance of ^{94}Mo.

5 New astrophysics prospects at NEAR using GEAR and CYCLING

The combination of neutron-TOF with activation measurements, when feasible, may deliver complementary and more

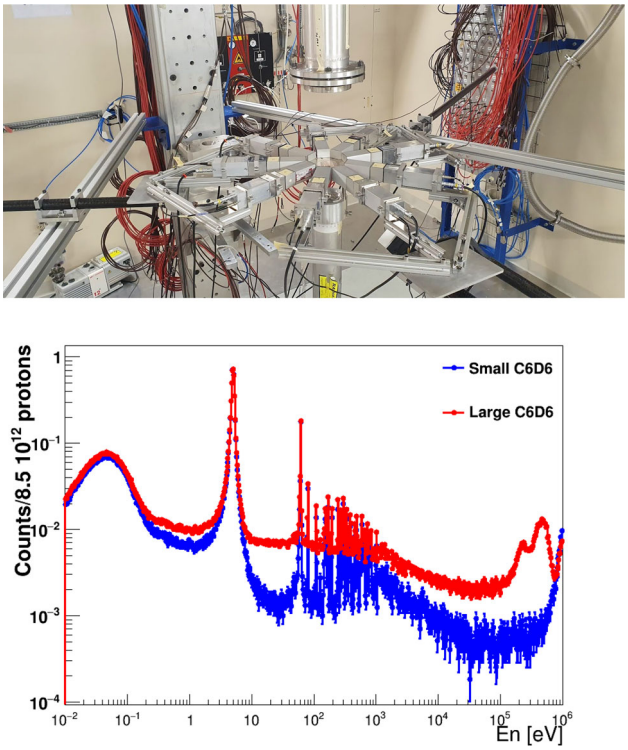

Fig. 4 (Top) Photograph of the capture setup based on an array of small-volume C_6D_6 detectors used for the ^{94}Nb(n,γ) experiment in 2022 at CERN n_TOF EAR2. (Bottom) Capture-spectra for ^{197}Au(n,γ) measured with a conventional large C_6D_6 detector and with a small volume C_6D_6 detector in EAR2. Both spectra have been normalized to the peak of the 4.9 eV resonance

accurate information on a specific cross section (see Table II in Ref. [10]). When applicable, the activation technique shows an unsurpassed sensitivity for the measurement of minuscule sample quantities, as it has been demonstrated for samples of only $\sim 10^{14}$ to 10^{15} atoms [87,88]. At high neutron-flux facilities, such as SARAF-LiLiT [89], the activation method can represent also an advantage for the measurement of highly radioactive samples [90], where the high sample-decay induced background would represent an important limitation for the TOF measurement.

Following this logic, one of the most recent efforts at n_TOF concerns the development of the neutron-activation station NEAR [91,92], aiming at exploiting the large neutron-fluxes in the proximity of the spallation target. Preliminary MC calculations [93] show the possibility of using suitable filters and moderation materials for producing quasi-Maxwellian neutron-energy spectra over a broad range between a few and several hundreds keV. A detailed description of the new NEAR installation will be reported in Ref. [92] and preliminary flux characterization measurements have been carried out recently [94]. Many of the latter measurements have been carried out at the Gamma-ray spectroscopy Experimental ARea (GEAR) of n_TOF, which is based on a CANBERRA HPGe detector GR5522 supplemented with convenient shielding [92]. This station is available for conventional neutron-activation measurements where γ-rays from the decay of the activation products with half-lives longer than a few hours are measured.

Because of the low duty cycle the average neutron fluence attainable at NEAR is expected to be comparable to the one available in the past at FZK [87] or currently at other activation facilities [95,96]. However, one of the unique features at NEAR will be the possibility to perform activation measurements on small samples of highly isotopically enriched (or even pure) material, which can be produced in sufficient quantities at the nearby ISOLDE [97] and MEDICIS facilities [98]. In addition to the GEAR station, there is another planned station for fast cyclic-activation measurements at NEAR called CYCLING [99]. The fast-cyclic activation technique was pioneered at FZK-Karslruhe [100], where it was applied to measure the neutron-capture cross section of several nuclides of relevance for nucleosynthesis in AGB stars, such as ^{107,109}Ag(n,γ) [100], ^{26}Mg(n,γ) [101], ^{50}Ti(n,γ) [102] and ^{19}F(n,γ) [88]. It is worth noting that measurements on isotopes with activation products with half-lives as short as $\sim$ 11 s (^{20}F) are accessible with this technique. The CYCLING station will enable the repetition of a short irradiation, followed by a rapid transport to a detector, where the measurement of the decay will take place and subsequently transported back to the irradiation position. This process is repeated for a number of cycles thus enhancing counting statistics and signal-to-background ratio for short-lived nuclei.

Thus, with the future combination of ISOLDE and GEAR-CYCLING it may become possible to access also direct neutron-capture measurements on several unstable nuclei of interest for the study of *s*-process branchings, and also for the more exotic intermediate *i*-process of nucleosynthesis [33]. The *i* process involves neutron capture at neutron densities of $10^{13} - 10^{16}$ cm^{-3}, in between the *s* and *r* processes. Recently, the *i* process attracted significant interest because it might explain the abundance pattern of a special kind of Carbon-Enhanced Metal-Poor stars (CEMPs), called CEMP-s/r [103]. The site of the *i*-process has been identified as the very late thermal pulse H-ingestion of post-AGB stars. Recent studies show also the relevance of this mechanism for the early generation of stars [104,105]. One case of interest in astrophysics is neutron capture on ^{135}Cs ($t_{1/2}$ = 2 Myr). The stellar neutron-capture rate of ^{135}Cs is relevant for the interpretation of the *s*-process branching at ^{134}Cs ($t_{1/2}$ = 2 yr) [10,106] and also for *i*-process nucleosynthesis, as discussed latter.

A suitable sample of ^{135}Cs could be ion-implanted at ISOLDE. After, characterization and activation at NEAR the decay of the activation product, ^{136}Cs ($t_{1/2}$=13 d), could be measured at the GEAR station or any other low-background

laboratory. The neutron capture of ^{135}Cs at $kT = 25$ keV has been already measured at FZK [106] and therefore this measurement could be a good benchmark case for the performance of the new installation. In addition, at NEAR the MACS could be also completed for other neutron energy ranges around $kT = 8$ keV and $kT = 90$ keV, where presently there is no experimental information available.

In the high neutron fluxes characteristic of the *i*-process it has been found [107] that variations in the neutron-capture rates of some specific radioactive isotopes around the $N = 82$ neutron-shell closure could affect elemental ratio predictions, involving the benchmark (observable) elements Ba, La and Eu [107]. Some of the involved reactions, such as ^{137}Cs(n, γ) may become accessible at NEAR. Commercial samples of ^{137}Cs ($t_{1/2}$ = 30 yr) are available and could be used for this measurement. A sample of about 2×10^{14} atoms and an activity of less than 200 kBq (662 keV γ-rays) could be a suitable option. Capture on ^{137}Cs leads either directly or via the detour of the shorter-lived ^{138m}Cs ($t_{1/2} = 3$ m) to the activation product ^{138g}Cs ($t_{1/2} = 33$ m) that emits a significant γ-ray intensity at 1.4 MeV. Owing to the short half-life it could be best measured at the CYCLING station.

As reported in Ref. [108], an AGB star experiencing *s*- or *i*-process nucleosynthesis would show very different isotopic fractions which, although challenging, could be inferred from observations. Thus, several isotopes of Ba, Nd, Sm and Eu may be used as tracers of *i*-process nucleosynthesis. For example, under *i*-process conditions the final abundance of ^{137}Ba is larger than that of ^{138}Ba. ^{138}Ba, with $N = 82$, has a very small neutron-capture cross section, acting as a bottleneck and therefore being copiously produced by the *s* process. The relatively large *i*-process abundance of ^{137}Ba is due to the decay of ^{137}Cs which, at variance with the *s* process, can be easily reached in *i*-process conditions. Therefore, the aforementioned ^{135}Cs(n, γ) and ^{137}Cs(n, γ) cross section measurements could provide a valuable input information for *i*-process models and observations. In addition, the measurement of the intermediate ^{136}Cs(n, γ) may become feasible, assuming that a sample with sufficient mass could be produced at ISOLDE and later activated at NEAR. After the neutron activation and sufficient waiting time to let the ^{136}Cs ($t_{1/2}$ = 13 d) in the sample decay, one could measure the activity of the activation product ^{137}Cs ($t_{1/2}$ = 30 yr) at the GEAR station. Other similar cases related to the *i*-process tracers discussed in Ref. [108] might be also accessible at NEAR, such as neutron capture on ^{144}Ce ($t_{1/2}$ = 285 d) leading to ^{145}Ce ($t_{1/2}$ = 3 m). However, the feasibility with CYCLING needs to be studied in detail owing to the γ-ray activity from neighbouring decays (mainly ^{144}Pr).

Finally, there are many other neutron-capture reactions of interest for the *i*-process, such as neutron capture on ^{66}Ni ($t_{1/2}$ = 55 h), which represents one of the major bottle-necks in *i*-process models [109] or neutron capture on ^{72}Zn ($t_{1/2}$ = 46 h) that determines the *i*-process abundance of Ge [109]. However, in these cases the conventional activation technique becomes prohibitive due to the large sample γ-ray activity, which typically exceeds 100 MBq for sample quantities of about 10^{12-13} atoms. For this reason, new ideas based on storage rings using either inverse kinematics with neutron sources [110,111] or indirect methods such as surrogate reactions [112,113], may represent the most promising alternative in the near future to obtain experimental information and to constrain the physical conditions of the stellar environments.

6 Summary and outlook

This article has presented a few technical contributions of n_TOF to the field of neutron-capture experiments of astrophysical interest. These works have been key, on the one hand, to address the accuracy of the measurements, and even enhance the systematic precision for this type of studies [34], an aspect which is closely connected with the 4–5% systematic error commonly required for reliable astrophysical interpretation of observational data or meteorites analysis [10,22,24]. Although historically, a large effort has been invested in reducing the intrinsic neutron-sensitivity of the detection apparatus, detailed MC calculations [25] showed that, in many situations, the background level is dominated by scattered neutrons, which are captured in the surroundings of the detectors, rather than in the detection system itself. In this respect, a novel i-TED detection system [65] based on γ-ray imaging has been developed, which allows one to attain a significant improvement in signal-to-background ratio for such specific cases in the keV-energy range of astrophysical interest [76]. This system has been employed at CERN n_TOF for the first measurement of the ^{79}Se(n, γ) cross section, which is one of the main branching points in the weak *s* process [10]. Further, for the measurement of highly-radioactive samples, such as ^{94}Nb described in Sect. 4, a new array of very small-volume C_6D_6 detectors was developed and implemented, which enabled also for a significant improvement in terms of signal-to-background ratio with respect to currently used C_6D_6 detectors. This measurement, carried out also in 2022 at CERN n_TOF, will help to shed light on isotopic Mo-anomalies observed in pre-solar SiC grains [86]. Future ideas and proposals at n_TOF are related to the new NEAR experimental area for exploiting also the neutron-activation technique in measurements of astrophysical interest. In this respect, current efforts to design a station for fast cyclic activation measurements (CYCLING) have also been presented. This installation could help to directly access for the first time to neutron-capture cross sections on radioactive isotopes, which are of great interest for the intermediate

neutron-capture process of nucleosynthesis and for the study of Carbon-Enhanced Metal-Poor stars.

Acknowledgements Part of this work has been carried out in the framework of a project funded by the European Research Council (ERC) under the European Union's Horizon 2020 research and innovation programme (ERC Consolidator Grant project HYMNS, with grant agreement No. 681740). The authors acknowledge support from the Spanish Ministerio de Ciencia e Innovación under grants PID2019-104714GBC21, FPA2017-83946-C2-1-P, FIS2015-71688-ERC, FPA-2016-77689-C2-1-R, RTI2018-098117-B-C21, CSIC for funding PIE-201750I26, European H2020-847552 (SANDA) and by funding agencies of participating institutes. For the purpose of open access, the author has applied a Creative Commons Attribution (CC BY) licence to any Author Accepted Manuscript version arising from this submission. In line with the principles that apply to scientific publishing and the CERN policy in matters of scientific publications, the n_TOF Collaboration recognises the work of V. Furman and Y. Kopatch (JINR, Russia), who have contributed to the experiment used to obtain the results described in this paper. This article belongs to a series of articles devoted to the memory of Franz Käppeler. The present work contains some of the developments where he was involved or witnessed and, some other contributions which came up more recently. In any case, all of them have undoubtedly benefited from the motivation and creativity that Franz inspired in all of us. Thank you Franz.

Data Availability Statement This manuscript has no associated data or the data will not be deposited. [Authors' comment: Pre-processed data is available from the Authors upon reasonable request.]

References

1. R.A. Alpher et al., The origin of chemical elements. Phys. Rev. **73**(7), 803–804 (1948)
2. R.A. Alpher, R.C. Herman, On the relative abundance of the elements. Phys. Rev. **74**(12), 1737–1742 (1948)
3. R.A. Alpher, A neutron-capture theory of the formation and relative abundance of the elements. Phys. Rev. **74**(11), 1577–1589 (1948)
4. R.A. Alpher et al., Thermonuclear reactions in the expanding universe. Phys. Rev. **74**(9), 1198–1199 (1948)
5. P.W. Merrill, Spectroscopic observations of stars of class. Astrophys. J. **116**, 21 (1952)
6. E.M. Burbidge et al., Synthesis of the elements in stars. Rev. Mod. Phys. **29**, 547–650 (1957)
7. A.G.W. Cameron, On the origin of the heavy elements. Astron. J. **62**, 9–10 (1957)
8. J.H. Gibbons, R.L. Macklin, Neutron capture and stellar synthesis of heavy elements. Science **156**(3778), 1039–1049 (1967)
9. R. Reifarth et al, Nuclear Astrophysics at DANCE. In R. C. Haight et al., editors, *International Conference on Nuclear Data for Science and Technology*, volume 769 of *American Institute of Physics Conference Series*, pp. 1323–1326 (2005)
10. F. Käppeler et al., The s process: Nuclear physics, stellar models, and observations. Rev. Mod. Phys. **83**(1), 157–194 (2011)
11. K. Langanke, Opportunities for nuclear astrophysics at FAIR. In *Journal of Physics Conference Series*, volume 966 of *Journal of Physics Conference Series*, pp. 012052 (2018)
12. A. Estrade, Beta-delayed neutron measurements for R-process isotopes with BRIKEN. In *APS Division of Nuclear Physics Meeting Abstracts*, volume 2019 of *APS Meeting Abstracts*, pp. SA.002 (2019)
13. C. Massimi et al., n_TOF: Measurements of Key Reactions of Interest to AGB Stars. Universe **8**(2), 100 (2022)
14. H. Schatz et al, Horizons: Nuclear Astrophysics in the 2020s and Beyond. arXiv e-prints, pp. (2022) arXiv:2205.07996
15. M. Pignatari et al., The weak s-process in massive stars and its dependence on the neutron capture cross sections. Astrophys. J. **710**(2), 1557–1577 (2010)
16. N. Colonna et al, The Nuclear Astrophysics program at n_TOF (CERN). In *European Physical Journal Web of Conferences*, volume 165 of *European Physical Journal Web of Conferences*, pp. 01014 (2018)
17. E. Chiaveri et al, Status and perspectives of the neutron time-of-flight facility n_TOF at CERN. In *European Physical Journal Web of Conferences*, volume 239 of *European Physical Journal Web of Conferences*, pp. 17001 (2020)
18. R. Esposito et al., Design of the third-generation lead-based neutron spallation target for the neutron time-of-flight facility at CERN. Phys. Rev. Acceler. Beams **24**(9), 093001 (2021)
19. I. Dillmann, The new KADoNiS v1.0 and its influence on the s-process. In *XIII Nuclei in the Cosmos (NIC XIII)*, pp. 57 (2014)
20. P. Neyskens et al., The temperature and chronology of heavy-element synthesis in low-mass stars. Nature **517**(7533), 174–176 (2015)
21. G. Cescutti et al., Uncertainties in s-process nucleosynthesis in low-mass stars determined from Monte Carlo variations. Mon. Not. R. Astron. Soc. **478**(3), 4101–4127 (2018)
22. G. Cescutti et al., The s-Process Nucleosynthesis in Low Mass Stars: Impact of the Uncertainties in the Nuclear Physics Determined by Monte Carlo Variations. In Nuclei in the Cosmos XV **219**, 297–300 (2019)
23. N. Nishimura et al, Sensitivity to neutron captures and β-decays of the enhanced s-process in rotating massive stars at low metallicities. In *Journal of Physics Conference Series*, volume 940 of *Journal of Physics Conference Series*, pp. 012051 (2018)
24. N. Nishimura et al, Impacts of nuclear-physics uncertainties in the s-process determined by Monte-Carlo variations. *arXiv e-prints*, pp. (2018) arXiv:1802.05836
25. P. Žugec et al., Experimental neutron capture data of ^{58}Ni from the CERN n_TOF facility. Phys. Rev. C **89**(1), 014605 (2014)
26. G. Giubrone et al., Measurement of the ^{5457}Fe(n,γ) Cross Section in the Resolved Resonance Region at CERN n_TOF. Nucl. Data Sheets **119**, 117–120 (2014)
27. C. Lederer et al., Ni62(n,γ) and Ni63(n,γ) cross sections measured at the n_TOF facility at CERN. Phys. Rev. C **89**(2), 025810 (2014)
28. C. Lederer et al., Erratum: ^{62}Ni(n,γ) and ^{63}Ni(n,γ) cross sections measured at the n_TOF facility at CERN [Phys. Rev. C 89, 025810 (2014)]. Phys. Rev. C **92**(1), 019903 (2015)
29. M. Weigand et al., ^{63}Cu(n,γ) cross section measured via 25 keV activation and time of flight. Phys. Rev. C **95**(1), 015808 (2017)
30. C.J. Prokop et al., Measurement of the ^{65}Cu(n,γ) cross section using the Detector for Advanced Neutron Capture Experiments at LANL. Phys. Rev. C **99**(5), 055809 (2019)

31. A. Laminack et al., Measurement of neutron-capture cross sections of ^{70,72}Ge using the DANCE facility. Phys. Rev. C **106**(2), 025802 (2022)
32. A. Wallner et al., Precise measurement of the thermal and stellar ^{54}Fe(n,γ)^{55}Fe cross sections via accelerator mass spectrometry. Phys. Rev. C **96**(2), 025808 (2017)
33. J.J. Cowan, W.K. Rose, Production of ^{14}C and neutrons in red giants. Astrophys. J. **212**, 149–158 (1977)
34. U. Abbondanno et al., New experimental validation of the pulse height weighting technique for capture cross-section measurements. Nucl. Inst. Methods Phys. Res. A **521**, 454–467 (2004)
35. R.L. Macklin, J.H. Gibbons, Capture-cross-section studies for 30–220-keV neutrons using a new technique. Phys. Rev. **159**, 1007–1012 (1967)
36. M.C. Moxon, E.R. Rae, A gamma-ray detector for neutron capture cross-section measurements. Nucl. Inst. Methods **24**, 445–455 (1963)
37. R.L. Macklin, Neutron capture measurements on radioactive ^{93}Zr. Astrophys. Space Sci. **115**(1), 71–83 (1985)
38. R.R. Winters, R.L. Macklin, Maxwellian-averaged Neutron Capture Cross Sections for 99Tc and 95–98Mo. Astrophys. J. **313**, 808 (1987)
39. F. Corvi et al., An experimental method for determining the total efficiency and the response function of a gamma-ray detector in the range 0.5-10 mev. Nucl. Instrum. Methods Phys. Res., Sect. A **265**(3), 475–484 (1988)
40. M. S. Coates et al, Can we do more to achieve accurate nuclear data? In K. H. Böckhoff, editor, *Nuclear Data for Science and Technology*, pp. 977–986, Dordrecht. Springer Netherlands (1983)
41. F. G. Perey, Status of the Parameters of the 1.15-keV Resonance of ^{56}Fe. In P. G. Young et al., editors, *Nuclear Data -for Basic and Applied Science*, 1, 1523 (1986)
42. J.L. Tain et al., Accuracy of the pulse height weighting technique for capture cross section measurements. J. Nucl. Sci. Technol. **39**(sup2), 689–692 (2002)
43. N. Yamamuro et al., Reliability of the weighting function for the pulse height weighting technique. Nucl. Inst. Methods **133**(3), 531–536 (1976)
44. S. Mizuno, Measurements of kev-neutron capture cross sections and capture gamma-ray spectra of 161162163dy. Journal of Nuclear Science and Technology, 36(6):493–507, et al., *Cited by: 59* (All Open Access, Bronze Open Access, 1999)
45. T. Katabuchi et al., Measurement of the neutron capture cross section of ^{99}Tc using ANNRI at J-PARC. EPJ Web of Conferences **146** (2017)
46. A. Borella et al., The use of C_6D_6 detectors for neutron induced capture cross-section measurements in the resonance region. Nucl. Inst. Methods Phys. Res. A **577**, 626–640 (2007)
47. C. Massimi et al., Au197(n,γ) cross section in the resonance region. Phys. Rev. C **81**(4), 044616 (2010)
48. F. Gunsing et al., Measurement of resolved resonances of ^{232}Th(n,γ) at the n_TOF facility at CERN. Phys. Rev. C **85**(6), 064601 (2012)
49. M.C. Moxon, J.B. Brisland, REFIT, A least squares fitting program for resonance analysis of neutron transmission and capture data computer code. Technical report
50. P. Schillebeeckx et al., Determination of resonance parameters and their covariances from neutron induced reaction cross section data. Nucl. Data Sheets **113**(12), 3054–3100 (2012)
51. J. Ren et al, Introduction of a C_6D_6 detector system on the Back-n of CSNS. In *European Physical Journal Web of Conferences*, volume 239 of *European Physical Journal Web of Conferences*, pp. 17021 (2020)
52. F.G. Perey et al, Responses of C_6D_6 and C_6F_6 gamma-ray detectors and the capture in the 1.15 keV resonance of ^{56}Fe. In MITO Copyright 1988 JAERI, editor, *Nuclear Data for Science and Technology*, volume 379-382 (1988)
53. C. Domingo-Pardo et al., New measurement of neutron capture resonances in Bi209. Phys. Rev. C **74**(2), 025807 (2006)
54. C. Domingo-Pardo et al., Resonance capture cross section of Pb207. Phys. Rev. C **74**(5), 055802 (2006)
55. C. Domingo-Pardo et al., Measurement of the neutron capture cross section of the s-only isotope Pb204 from 1 eV to 440 keV. Phys. Rev. C **75**(1), 015806 (2007)
56. C. Domingo-Pardo et al., Measurement of the radiative neutron capture cross section of Pb206 and its astrophysical implications. Phys. Rev. C **76**(4), 045805 (2007)
57. S. Agostinelli et al., Geant4-a simulation toolkit. Nucl. Instrum. Methods Phys. Res., Sect. A **506**(3), 250–303 (2003)
58. F. Bečvář, Simulation of cascades in complex nuclei with emphasis on assessment of uncertainties of cascade-related quantities. Nucl. Instrum. Methods Phys. Res., Sect. A **417**(2), 434–449 (1998)
59. J.L. Tain, D. Cano-Ott, The influence of the unknown de-excitation pattern in the analysis of β-decay total absorption spectra. Nucl. Inst. Methods Phys. Res. A **571**(3), 719–727 (2007)
60. S. Valenta et al., Examination of photon strength functions for ^{162,164}Dy from radiative capture of resonance neutrons. Phys. Rev. C **96**(5), 054315 (2017)
61. J. Moreno-Soto et al., Constraints on the dipole photon strength for the odd uranium isotopes. Phys. Rev. C **105**(2), 024618 (2022)
62. R. Plag et al., An optimized C $_6$D $_6$ detector for studies of resonance-dominated (n,γ) cross-sections. Nucl. Inst. Methods Phys. Res. A **496**, 425–436 (2003)
63. M. Igashira et al., Nuclear data study at j-parc bl04. Nucl. Instrum. Methods Phys. Res., Sect. A **600**(1), 332–334 (2009)
64. T. Katabuchi et al., Pulse-width analysis for neutron capture cross-section measurement using an nai(tl) detector. Nucl. Instrum. Methods Phys. Res., Sect. A **764**, 369–377 (2014)
65. C. Domingo-Pardo, i-TED: A novel concept for high-sensitivity (n,γ) cross-section measurements. Nucl. Inst. Methods Phys. Res. A **825**, 78–86 (2016)
66. G. Tagliente et al., The ^{93}Zr(n,γ) reaction up to 8 keV neutron energy. Phys. Rev. C **87**(1), 014622 (2013)
67. P. Žugec et al., An improved method for estimating the neutron background in measurements of neutron capture reactions. Nucl. Inst. Methods Phys. Res. A **826**, 80–89 (2016)
68. D.L. Pérez Magán et al., First tests of the applicability of γ-ray imaging for background discrimination in time-of-flight neutron capture measurements. Nucl. Inst. Methods Phys. Res. A **823**, 107–119 (2016)
69. V. Schönfelder et al., A telescope for soft gamma ray astronomy. Nucl. Inst. Methods **107**, 385–394 (1973)
70. S.J. Wilderman et al., Fast algorithm for list mode back-projection of Compton scatter camera data. IEEE Trans. Nucl. Sci. **45**, 957–962 (1998)
71. ERC-Consolidator Grant Agreement No. 681740, HYMNS, High-sensitivitY Measurements of key stellar Nucleo-Synthesis reactions (2016-2022), PI: C. Domingo Pardo
72. P. Olleros et al., On the performance of large monolithic $LaCl_3$(Ce) crystals coupled to pixelated silicon photosensors. J. Instrum. **13**, P03014 (2018)
73. V. Babiano et al., γ-Ray position reconstruction in large monolithic $LaCl_3$(Ce) crystals with SiPM readout. Nucl. Inst. Methods Phys. Res. A **931**, 1–22 (2019)
74. J. Balibrea-Correa et al., Machine learning aided 3D-position reconstruction in large $LaCl_3$ crystals. Nucl. Instrum. Methods Phys. Res., Sect. A **1001**, 165249 (2021)
75. V. Babiano et al., First i-TED demonstrator: A Compton imager with Dynamic Electronic Collimation. Nucl. Inst. Methods Phys. Res. A **953**, 163228 (2020)

76. V. Babiano-Suárez et al., Imaging neutron capture cross sections: i-TED proof-of-concept and future prospects based on Machine-Learning techniques. Eur. Phys. J. A **57**(6), 197 (2021)
77. A. Di Francesco et al., TOFPET 2: A high-performance circuit for PET time-of-flight. Nucl. Inst. Methods Phys. Res. A **824**, 194–195 (2016)
78. J. Lerendegui-Marco et al, First measurement of the *s*-process branching ^{79}Se(n, γ). Technical report, CERN-INTC-2020-065; INTC-P-580; http://cds.cern.ch/record/2731962 (2021)
79. N.M. Chiera et al., Preparation of PbSe targets for ^{79}Se neutron capture cross section studies. Nucl. Inst. Methods Phys. Res. A **1029**, 166443 (2022)
80. G. Walter et al., The s-process branching at Se-79. Astrophys. J. **167**(1), 186–199 (1986)
81. J. Lerendegui-Marco et al., Geant4 simulation of the n_TOF-EAR2 neutron beam: Characteristics and prospects. Eur. Phys. J. A **52**(4), 100 (2016)
82. P. Koehler, Comparison of white neutron sources for nuclear astrophysics experiments using very small samples. Nucl. Instrum. Methods Phys. Res., Sect. A **460**(2), 352–361 (2001)
83. V. Alcayne et al, (The n_TOF Collaboration). The segmented total-energy detector s-TED. *(in preparation)* (2022)
84. J. Balibrea-Correa et al, (The n_TOF Collaboration). An array of low-volume total-energy detectors for enhanced sensitivity measurements at CERN n_TOF EAR2. *(in preparation)* (2022)
85. J.I. Moench et al., Materials. Trans. JIM **41**, 67–70 (2000)
86. M. Lugaro et al., Isotopic compositions of strontium, zirconium, molybdenum, and barium in single presolar SiC grains and asymptotic giant branch stars. Astrophys. J. **593**(1), 486–508 (2003)
87. R. Reifarth et al., Stellar neutron capture on promethium: Implications for thes-process neutron density. Astrophys J **582**(2), 1251–1262 (2003)
88. E. Uberseder et al., New measurements of the F19(n,γ)F20 cross section and their implications for the stellar reaction rate. Phys. Rev. C **75**(3), 035801 (2007)
89. M. Tessler et al., Stellar s -process neutron capture cross sections on ^{78,80,84,86}Kr determined via activation, atom trap trace analysis, and decay counting. Phys. Rev. C **104**(1), 015806 (2021)
90. C. Guerrero et al., Neutron capture on the s -process branching point Tm 171 via time-of-flight and activation. Phys. Rev. Lett. **125**(14), 142701 (2020)
91. M. Ferrari et al, Design development and implementation of an irradiation station at the neutron time-of-flight facility at CERN. (2022) *arXiv e-prints*, pp. arXiv:2202.12809
92. N. Patronis et al, The CERN n_TOF NEAR station for astrophysics- and application-related neutron activation measurements. (2022) *arXiv e-prints*, pp. arXiv:2209.04443
93. A. Mengoni et al, The new n_TOF NEAR Station. Technical report, CERN-INTC-2020-073 ; INTC-I-222; http://cds.cern.ch/record/2737308 (2020)
94. E. Stamati et al, Neutron capture cross section measurements by the activation method at the n_TOF NEAR Station. Technical report, CERN-INTC-2022-008 ; INTC-P-623; http://cds.cern.ch/record/2798978 (2022)
95. S. Alzubaidi et al., The Frankfurt neutron source FRANZ. Eur. Phys. J. Plus **131**(5), 124 (2016)
96. B. Fernández et al, HiSPANoS facility and the new neutron beam line for TOF measurements at the Spanish National Accelerator Lab (CNA). In *Journal of Physics Conference Series*, volume 1643 of *Journal of Physics Conference Series*, pp. 012033 (2020)
97. J. Ballof et al., The upgraded ISOLDE yield database - A new tool to predict beam intensities. Nucl. Inst. Methods Phys. Res. B **463**, 211–215 (2020)
98. V.M. Gadelshin et al., First laser ions at the CERN-MEDICIS facility. Hyperfine Interact. **241**(1), 55 (2020)
99. J. Lerendegui-Marco et al, Measurement of the radiation background at the n TOF NEAR facility to study the feasibility of cyclic activation experiments. Technical report, CERN-INTC-2022-018 ; INTC-I-241. http://cds.cern.ch/record/2809131 (2022)
100. H. Beer et al., The fast cyclic neutron activation technique at the karlsruhe 3.75 mv van de graaff accelerator and the measurement of the 107,109ag(n,)108,110ag cross sections at kt = 25 kev. Nucl. Instrum. Methods Phys. Res., Sect. A **337**(2), 492–503 (1994)
101. P. Mohr et al., Neutron capture of ^{26}Mg at thermonuclear energies. Phys. Rev. C **58**, 932–941 (1998)
102. P.V. Sedyshev et al., Measurement of neutron capture on ^{50}Ti at thermonuclear energies. Phys. Rev. C **60**, 054613 (1999)
103. M. Hampel et al., The intermediate neutron-capture process and carbon-enhanced metal-poor stars. Astrophys. J. **831**(2), 171 (2016)
104. A. Heger, S.E. Woosley, The nucleosynthetic signature of population III. Astrophys. J. **567**(1), 532–543 (2002)
105. A. Frebel et al., Nucleosynthetic signatures of the first stars. Nature **434**(7035), 871–873 (2005)
106. N. Patronis et al., Neutron capture studies on unstable ^{135} Cs for nucleosynthesis and transmutation. Phys. Rev. C **69**(2), 025803 (2004)
107. M. G. Bertolli et al, Systematic and correlated nuclear uncertainties in the i-process at the neutron shell closure N = 82. *arXiv e-prints*, pp. (2013) arXiv:1310.4578
108. A. Choplin et al., The intermediate neutron capture process. I. Development of the i-process in low-metallicity low-mass AGB stars. Astron. Astrophys. **648**, A119 (2021)
109. J.E. McKay et al., The impact of (n,γ) reaction rate uncertainties on the predicted abundances of i-process elements with 32 $\leq$ Z $\leq$ 48 in the metal-poor star HD94028. Mon. Not. R. Astron. Soc. **491**(4), 5179–5187 (2020)
110. R. Reifarth et al., Spallation-based neutron target for direct studies of neutron-induced reactions in inverse kinematics. Phys. Rev. Acceler. Beams **20**(4), 044701 (2017)
111. S. Mosby et al, Direct studies of neutron-induced reactions in inverse kinematics. In *APS Division of Nuclear Physics Meeting Abstracts*, volume 2017 of *APS Meeting Abstracts*, pp. JC.008 (2017)
112. R. Pérez Sánchez et al., Simultaneous determination of neutron-induced fission and radiative capture cross sections from decay probabilities obtained with a surrogate reaction. Phys. Rev. Lett. **125**(12), 122502 (2020)
113. B. Jurado et al, Direct and Indirect Measurements of Neutron Induced Cross Sections at Storage Rings. In *10th International Conference on Nuclear Physics at Storage Rings (STORI'17)*, 011001 (2021)